Acta Metallurgica, Vol. 28, pp. 989 to 998

0001-6160/80/0701-0989$02.00/0

THE DEFORMATION MICROSTRUCTURE OF THE Ni–Ni_4Mo SYSTEM

† L. A. NESBIT and ‡ D. E. LAUGHLIN

† Senior Associate Engineer, IBM-Burlington, Essex Junction, Vermont 05452 U.S.A.
‡ Department of Metallurgy & Materials Science, Carnegie-Mellon University, Pittsburgh, Pennsylvania 15213.

(*Received* 23 *October* 1979)

Abstract—The deformation microstructure of stoichiometric Ni_4Mo and of an off-stoichiometric Ni–Ni_4Mo alloy are examined via transmission electron microscopy. In general, the Ni_4Mo superlattice dislocation does not form in either alloy, although one instance is documented in which the superlattice dislocation was found in the off-stoichiometric alloy. Stacking faults and deformation twins are prevalent in the stoichiometric alloy and in the off-stoichiometric alloy containing large Ni_4Mo precipitates. Although twinning is not a preferred deformation mode for many ordered alloys, a twinning mechanism is proposed which explains the prevalence of such twins in the Ni–Ni_4Mo alloy system.

Résumé—Nous avons étudié par microscopie électronique en transmission la microstructure de déformation de Ni_4Mo stoechiométrique et de l'alliage Ni–Ni_4Mo non steochiométrique. D'une manière générale, on n'observe pas de superdislocations dans les deux alliages (même si nous en avons observé une fois dans l'alliage non stoechiométrique). Dans l'alliage stoechiométrique, on observe de nombreux défauts d'empilement et de nombreuses macles mécaniques, alors que l'alliage non stoechiométrique contient de gros précipités de Ni_4Mo. Bien que le maclage ne soit pas le mode de déformation principal de nombreux alliages ordonnés, nous proposons un mécanisme de maclage pour expliquer la prépondérence de telles macles dans le système Ni–Ni_4Mo.

Zusammenfassung—Die Verformungsmikrostruktur wurde in der stöchiometrischen Legierung Ni_4Mo und in der nicht-stöchiometrischen Legierung Ni–Ni_4Mo mittels Durchstrahlungselektronenmikroskopie untersucht. Im allgemeinen bilden sich Versetzungen der Ni_4Mo-Überstruktur in beiden Legierungen nicht aus, obwohl ein Fall vorliegt, bei dem Überstrukturversetzungen in der nicht-stöchiometrischen Legierung auftefunden wurden. Stapelfehler und Verformungszwillinge wiegen vor in der stöchiometrischen Legierung und in der nicht-stöchiometrischen Legierung, die große Ni_4Mo-Ausscheidungen enthält. Wenn auch Zwillingsbildung nicht die wesentlichste Verformungsart bei vielen geordneten Legierungen ist, so wird doch ein Zwillingsmechanismus vorgeschlagen, der das Überwiegen solcher Zwillinge im Legierungssystem Ni–Ni_4Mo erklärt.

INTRODUCTION

Recent investigations of the Ni–Mo system have concentrated primarily upon the mechanisms whereby the ordered Ni_4Mo phase precipitates from the disordered nickel–molybdenum solid solution. Most of this research has been directed towards the stoichiometric alloy Ni_4Mo [1–6], although more recent studies have considered certain nickel-rich off-stoichiometric alloys as well [7, 8]. Despite this emphasis on the transformation mode, only a few investigators have considered the deformation microstructure and the strengthening mechanisms of either the single phase Ni_4Mo ordered alloy [9–12], or of a two-phase Ni–Ni_4Mo alloy [13].

The purpose of this paper is to document and to discuss the deformation microstructure of the fully ordered Ni_4Mo alloy and of an off-stoichiometric Ni–Ni_4Mo alloy.

Before proceeding to the main body of the paper, a brief review of the Ni_4Mo structure and of the deformation characteristics of ordered alloys is appropriate. The ordered Ni_4Mo structure (Dla, I4/m) is based upon a body-centered tetragonal Bravais lattice, and is a crystallographic derivative of the parent f.c.c. lattice (Al, Fm3m). The Ni_4Mo structure contains ten atoms per unit cell: two Mo atoms and eight Ni atoms. The first and second nearest neighbor atoms of each Ni and Mo atom in the Ni_4Mo structure are given in Table 1. For further details concerning the crystallography of the Ni_4Mo structure, the reader is referred to other articles which review this subject [2, 5, 9].

Throughout this paper, the Greek letters α and β refer to the Ni terminal solid solution and to the ordered Ni_4Mo phase respectively. When these letters appear in conjunction with Miller indices and direction indices, they refer to the face-centered cubic lattice and to the ordered Ni_4Mo structure respectively.

In ordered alloys, the defect structure of major interest is the superlattice dislocation (or simply the superdislocation) and its attendant planar defects. The total Burgers vector of the superdislocation must necessarily be equal to a superlattice translation vec-

Table 1. First and second near-neighbor (N.N.) atoms of the Ni and Mo atoms in the Ni_4Mo structure

Central Atom	1st N.N.		2nd N.N.	
	Ni	Mo	Ni	Mo
Mo	12	0	4	2
Ni	9	3	5	1

tor. For the Dla structure, the equivalent atomic positions are located at the $(0, 0, 0)_{\alpha,\beta}$ and at the $(\frac{1}{2}, \frac{1}{2}, \frac{1}{2})_\beta$ or $(1, \frac{1}{2}, \frac{1}{2})_\alpha$ positions. Since the ordered Ni_4Mo phase has a $(c/a)_\alpha$ ratio only slightly less than one (0.986), the slip planes are expected to be the $\{111\}_\alpha$ or equivalently the $\{121\}_\beta$ planes, and the close-packed directions to be the $\langle 110\rangle_\alpha$ or $\langle 120\rangle_\beta$ directions. Fig. 1 shows the $(111)_\alpha$ plane of the fully ordered Ni_4Mo structure. Notice that in each of the close-packed $\langle 110\rangle_\alpha$ directions that five $\frac{1}{2}\langle 110\rangle_\alpha$ displacements are required to bring the ordered lattice back into coincidence with itself, as previously pointed out by Ruedl *et al.* [9]. Although this is a rather large superdislocation, it has the advantage that all of the component unit dislocations have identical Burgers vectors. Hence five unit dislocations of $\vec{\mathbf{b}} = \frac{1}{2}\langle 110\rangle_\alpha$ could conceivably emanate from the same source. Other superdislocations composed of fewer unit dislocations are geometrically possible, as illustrated by Ruedl *et al.* [9]. Such superdislocations would have a lower self-energy but the Burgers vectors of the unit dislocations would not be identical.

Although twinning is not a common deformation mode of ordered alloys, deformation twins are found in both the stoichiometric and off-stoichiometric alloys of the Ni–Ni_4Mo system. Laves [14] first recognized that deformation twins generally fail to form in ordered alloys since the mechanism which produces a twin in a disordered alloy does not necessarily produce a twin in the ordered structure, in the strict crystallographic sense of the word 'twin.' In particular, he demonstrated that the reported 'twins' in Fe_3Be (DO_3, Fm 3m) were not true twins, since they were of a different crystal structure (orthorhombic) than the DO_3 (cubic) structure. Nevertheless, twins can form in many ordered alloys if the twinning mechanism is different from that of the disordered alloy. For example, in Cu_3Au a true twin can be formed by displacements of $\vec{\mathbf{b}} = (a/3)\langle 11\bar{2}\rangle$ on each successive close-packed plane. Such displacements are equivalent to forming extrinsic stacking faults on every $\{111\}$ plane or intrinsic stacking faults on every other $\{111\}$ plane.

In the Ni_4Mo structure, (Dla) a true twin can be produced by the normal f.c.c. deformation twinning mode. That is, the movement of an $(a/6)\langle 112\rangle$ partial dislocation on each successive close-packed plane may yield a twinned region which retains the Dla crystal structure. Details of this deformation mode are elucidated below.

EXPERIMENTAL PROCEDURE

The stoichiometric Ni_4Mo alloy was prepared from powders of each of the component metals; each metal powder having an initial purity of 99.9%. After the powders were mixed and arc-melted, the ensuing alloy was homogenized at 1425 K in an inert atmosphere. The alloy was then cold-rolled into sheet form approximately 0.25 mm thick, and then annealed at 1273 K. At the termination of this second anneal, the stoichiometric alloy was furnace cooled to 1108 K (30 K below the critical ordering temperature) and aged for 3×10^4 min. A final deformation of 1% was induced into the alloy by cold-rolling it at room temperature.

The off-stoichiometric alloy was prepared by the International Nickel Company (INCO) at a composition of Ni–15.6 at.% Mo. This alloy was machined into standard quarter-inch diameter tensile specimens, in accordance with ASTM standard E8-69 [15], and then solution treated at 1273 K, prior to down-quenching the alloy to 948 K or 1025 K for various aging times up to 10,000 min. The tensile specimens were pulled to fracture on an Instron Universal Testing Instrument at a strain rate of $3.3 \times 10^{-4}\,s^{-1}$. In those tensile specimens which proved to be extremely brittle after the final aging anneal, a plastic strain of 3–4% was induced by deforming the specimens in compression.

The alloy microstructures were examined with a JEM 100B transmission electron microscope,

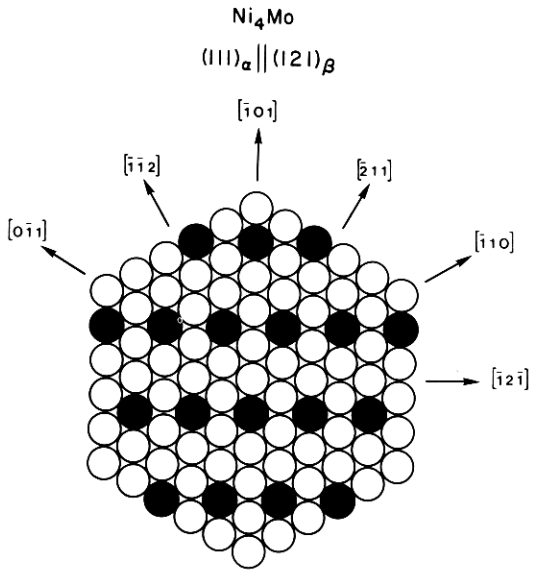

Fig. 1. The close-packed plane of fully ordered Ni_4Mo. Every fifth atom in the close-packed directions, $\langle 110\rangle_\alpha$, is a Mo atom. Filled circles indicate Mo atoms, and open circles designate Ni atoms.

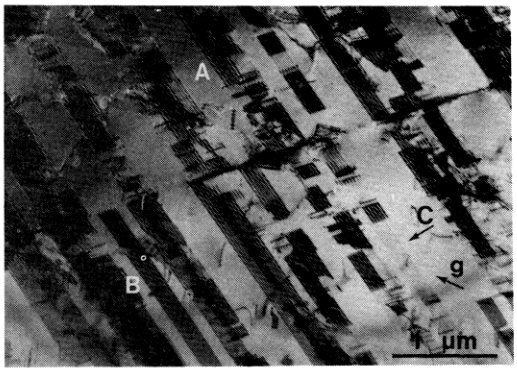

Fig. 2. Stacking faults in fully ordered Ni_4Mo, deformed 1%, as observed along the $[101]_\gamma$ zone axis with $\mathbf{g} = [\bar{1}11]_\gamma$.

equipped with a double-tilt stage. The TEM specimens were electropolished via the twin-jet technique in a solution of 1/3 nitric acid and 2/3 methanol at 248 K.

RESULTS

The deformation microstructure of Ni_4Mo

The deformation microstructure of fully ordered Ni_4Mo, deformed one percent by rolling, contains numerous stacking faults with widely separated partial dislocations.

As shown in Fig. 2, the stacking faults are often several hundred nanometers wide, which is indicative of a low stacking fault energy. When individual stacking faults were found, such as those designated by the letters A and B in Fig. 2, two techniques of analysis were employed in order to confirm the nature of the faults. The first method, as developed by Gevers *et al.* [16] makes use of the fringe contrast in a dark-field micrograph of the stacking fault, along with the relative direction of the operating g-vector. The second technique of fault analysis, as described by Art *et al.* [17] is based upon a comparison of the fringe contrast in both the bright and dark-field micrographs of the stacking faults. The advantage of this latter technique is that the direction of the tilt of the stacking fault in the foil is inherently determined, as well as the nature of the stacking fault. In Fig. 2, if the origin of the arrow marked C is placed at the center of a given stacking fault, it will point towards the side of the stacking fault that intersects the top of the foil. The results from applying both of the above techniques confirm that the stacking faults in Fig. 2 are intrinsic in nature.

In some grains several stacking faults overlap one another, making analysis of these stacking faults extremely difficult. See Fig. 3. When individual or non-overlapping faults were found they also were determined to be intrinsic in nature. The stacking faults in Fig. 3 are viewed under the diffracting conditions of $\vec{n} = [101]_\gamma$ and $\vec{g} = [\bar{1}11]_\gamma$. Notice the numerous discontinuities in the fringe contrast along these stacking faults. When this same grain is examined with an operating $\vec{g}$ of $\vec{g} = [\bar{2}02]_\gamma$, dislocations are observed which correspond to the discontinuities in the fringe contrast. See Fig. 4 and compare it with Fig. 3. These dislocations are most likely partial dislocations with Burgers vectors of $1/6[\bar{2}\bar{1}1]_\gamma$ or $1/6[1\bar{1}\bar{2}]_\gamma$. The $1/6[12\bar{1}]_\gamma$ partial dislocation is not observed under the given diffracting conditions.

When this same grain is rotated to $\vec{n} = [110]_\gamma$, the overlapping stacking faults are observed on edge in direct space, and they are found to produce extra reflections which are twin related to the fundamental reflections in reciprocal space. See Figs 5a and 5c. In Fig. 5c the twin axis is the $[1\bar{1}1]_\gamma$ direction. Only one set of extra twin reflections is observed on the diffracting pattern, which implies that twinning has taken place on only one of two possible $\{111\}_\gamma$ planes that diffract in this reciprocal lattice plane. This implication is confirmed by imaging a twin reflection in dark-field (Fig. 5b) and comparing it with the corresponding bright-field image (Fig. 5a). Since the twinned regions are relatively thin, the twin reflections are elongated in the $[111]_\gamma$ direction, and in fact a

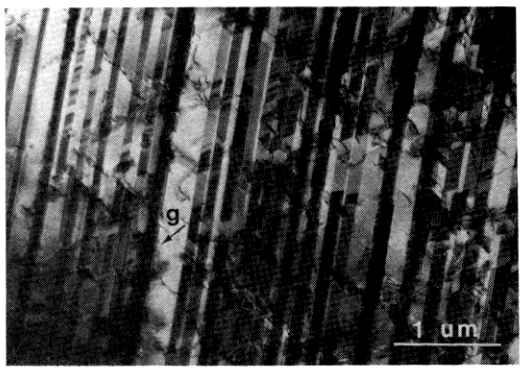

Fig. 3. Overlapping stacking faults in fully ordered Ni_4Mo, deformed 1%, as observed along the $[101]_\gamma$ zone axis with $\mathbf{g} = [\bar{1}11]_\gamma$.

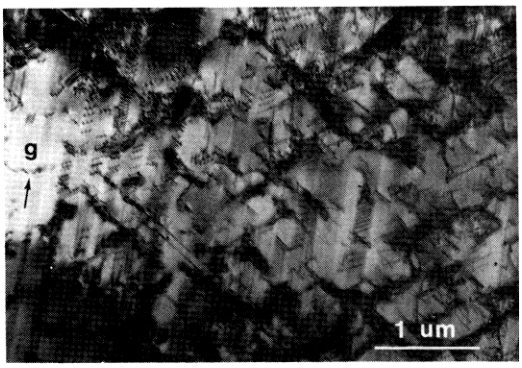

Fig. 4. Fully ordered Ni_4Mo deformed 1% as observed along the $[101]_\gamma$ zone axis for $\mathbf{g} = [\bar{2}02]_\gamma$. The area of this micrograph corresponds to approximately the same area as observed in Fig. 3.

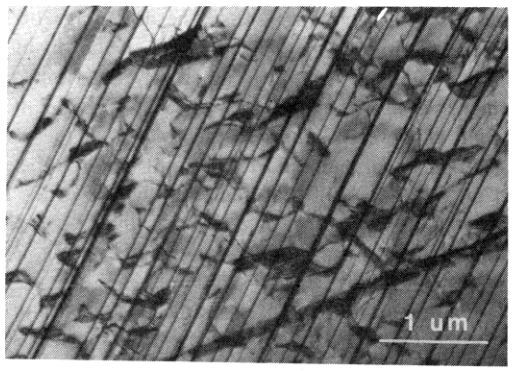

(a)

(b)

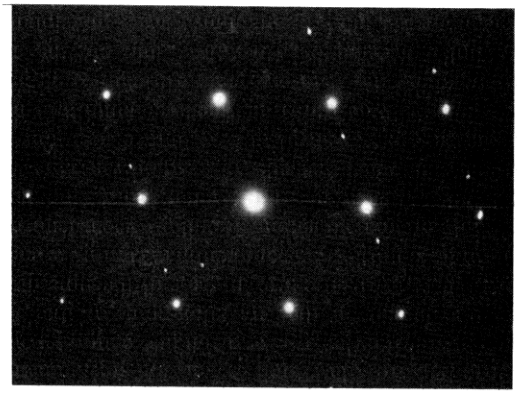

(c)

Fig. 5. Fully ordered Ni_4Mo deformed 1% as observed along the $[110]_z$ zone axis in (a) bright-field and (b) dark-field by imaging the twin reflections along the $[1\bar{1}1]_z$ direction in the corresponding diffraction pattern (c).

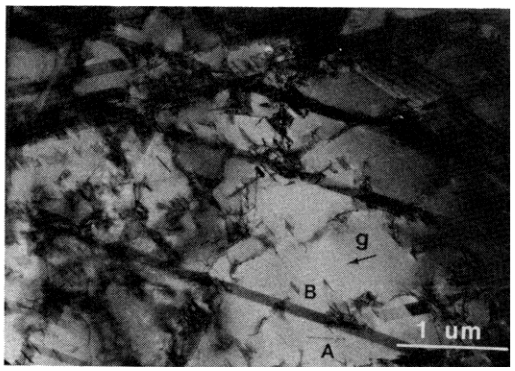

(a)

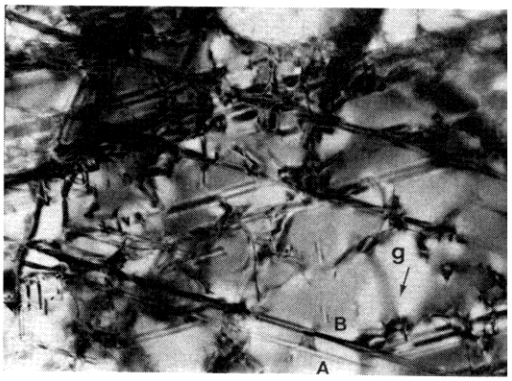

(b)

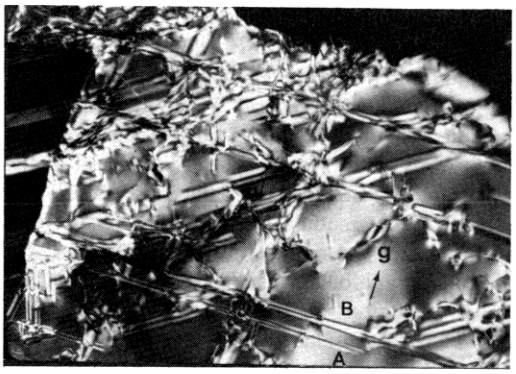

(c)

Fig. 6. Fully ordered Ni_4Mo, deformed 1%, as observed along the $[100]_z$ zone axis. The directions of the appropriate g-vectors are indicated in the respective micrographs. (a) $\mathbf{g} = [020]_z$; (b) $\mathbf{g} = 1/5[042]_z$; and (c) $\mathbf{g} = -1/5[042]_z$.

faint streak of diffracted intensity lies in this same direction.

A comparison of Figs 5a and 3 indicates that a one-to-one correspondence exists between the twins in Fig. 5a and the overlapping stacking faults in Fig. 3. Thus the deformation twins are composed of a series of overlapping intrinsic stacking faults.

When the microstructure of deformed Ni_4Mo is observed along either the $\langle 100 \rangle_z$, or the $\langle 112 \rangle_z$ zone axes, it is possible to view the antiphase boundaries between unit dislocations by imaging the microstructure with a g-vector of $\vec{\mathbf{g}} = 1/5\langle 420 \rangle_z$. The micrographs in Fig. 6 are all of approximately the same area of the microstructure, but each micrograph is taken under different diffracting conditions. Figure 6a shows stacking faults between many, but not all of the dislocations. For instance, the dislocation just above the letter A in this figure is not associated with a stacking fault; whereas a stacking fault is observed just below the letter B in this same micrograph. Figures 6b and 6c display the antiphase boundaries as observed in bright-field ($\vec{\mathbf{g}} = 1/5[042]_z$) and in the

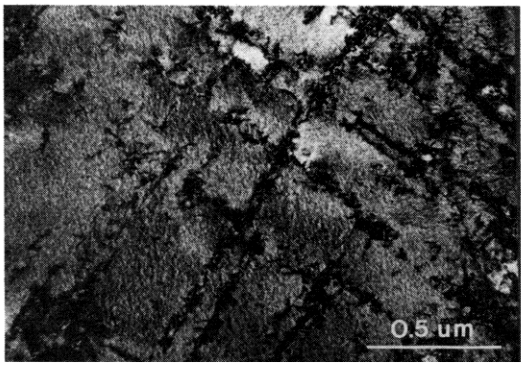

(a)

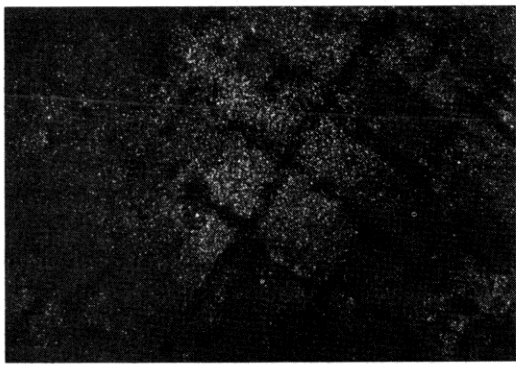

(b)

Fig. 7. The deformation microstructure of the off-stoichiometric alloy aged at 675°C (948 K) for 100 min and subsequently pulled to fracture, as observed along the $[001]_\alpha$ zone axis. (a) Bright-field image produced under multiple-beam diffracting conditions. (b) Dark-field micrograph produced by imaging both superlattice reflections on the (001) diffraction pattern.

dark-field ($\vec{g} = -1/5[042]_\alpha$) micrographs, respectively. In these latter two micrographs, an antiphase boundary is associated with the dislocation at A, as well as with the stacking fault at B. In fact, an antiphase boundary is associated with nearly every dislocation and stacking fault throughout the entire deformation microstructure. The fringe contrast of the antiphase boundaries APB's is characteristic of α-fringes [18] and it is similar to that found by Ruedl *et al.* [8] for translational APB's. Such a translational APB is expected to be associated with a unit dislocation in the ordered Ni_4Mo structure as opposed to an antiparallel twin or a perpendicular twin boundary.

In general, the dislocations in the deformed Ni_4Mo alloy do *not* exist in groups, with a characteristic number of dislocations in each group, as might be expected in an ordered alloy. Thus the deformation of ordered Ni_4Mo at room temperature does not result in the formation of superlattice dislocations. Instead the deformed microstructure is characterized by intrinsic stracking faults, by deformation twins composed of intrinsic stacking faults, and by individual unit dislocations, which do not appear to act in concert with one another.

The deformation microstructure of an off-stoichiometric alloy

The deformation microstructure of the off-stoichiometric alloy in which no ordered Ni_4Mo precipitates are present, but only short range order, displays neither stacking faults nor pairs or groups of dislocations, as might be expected of alloys with short-range order (SRO). The dislocations that are present are found in broad slip bands, with the slip planes along the traces of the $\{111\}_\alpha$ planes. In reciprocal space, the short-range order reflections are still present after deformation, albeit they are fainter than the same reflections from an undeformed region of the same specimen.

Specimens aged at 948 K (675°C), with a corresponding precipitate size of 7.5 nm are void of stacking faults and any identifiable superdislocations. Most of the unit dislocations are congregated into a relatively few narrow slip bands as shown in Fig. 7a. The superlattice dark-field micrograph in Fig. 7b reveals comparatively few Ni_4Mo precipitates in the slip bands. In reciprocal space, the superlattice reflections are more diffuse than those from an undeformed region of the same specimen.

The decrease in the intensity of the SRO reflections in specimens in which only short-range order is present, and the increase in the diffuseness of the superlattice reflections in specimens with small precipitates, results from dislocations destroying the respective types of order. In the latter instance, the increase in the diffuseness of the superlattice reflections indicates that the dislocations are cutting the precipitates and effectively reducing their size, rather than looping around the precipitates. Some of the ordered precipitates in the slip bands are cut to the extent of being destroyed, as evidenced by their diminished number in the slip bands relative to the undeformed matrix.

Certain heat treatments result in extremely brittle specimens, so as to preclude plastic deformation in tension and to necessitate deformation in compression. An example of such a heat treatment is an aging time of 10,000 min at a temperature of 1023 K (750°C), which produces precipitates 80–100 nm in size as measured perpendicular to the Dla c-axis. A specimen which had been aged in this manner was deformed in compression by 3.5%. The resulting microstructure contains stacking faults which are unimpeded and undeviated by the presence of the precipitates. See Fig. 8. The stacking faults seem to nucleate at grain boundaries, since the stacking faults often extend from a grain boundary into the grain and terminate either with a partial dislocation within the grain or at the intersection with another stacking fault. Analysis of the stacking faults in order to determine their specific nature (i.e. intrinsic or extrinsic) was hindered by the fact that the faults pass through both the matrix and the precipitates, which consequently disrupts the corresponding fringe contrast.

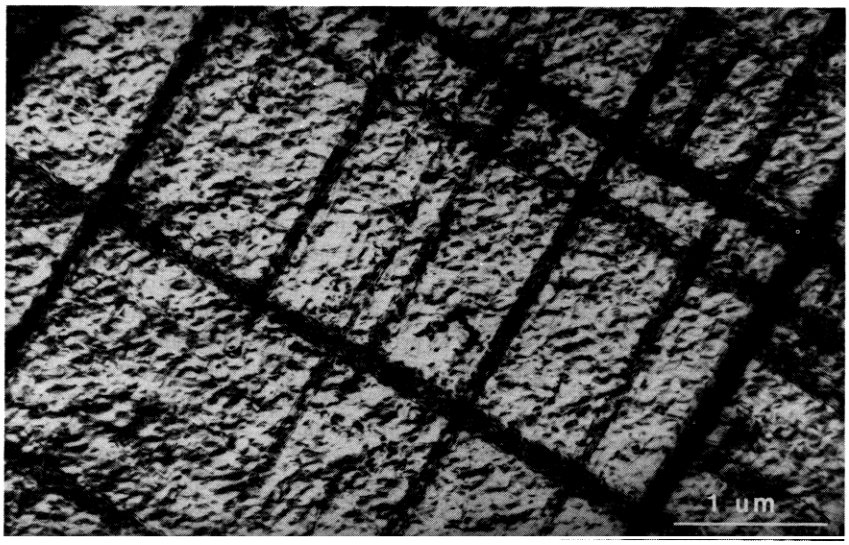

Fig. 8. The deformation microstructure of the off-stoichiometric alloy aged at 750°C (1023 K) for 10,000 min and subsequently deformed in compression by 3.5%. Stacking faults are observed along the traces of the $\{111\}_\alpha$ planes as viewed along the $[001]_\alpha$ zone axis.

When the above specimen is tilted to the $[110]_\alpha$ zone axis, streaks are observed in the $[1\bar{1}1]_\alpha$ direction, with extra spots or reflections along these streaks. These extra reflections are twin related to the fundamental reflections across the $(1\bar{1}1)_\alpha$ reciprocal space plane, and they are identical to the twin reflections from deformed Ni_4Mo (see Fig. 5c). The bright- and dark-field micrographs of the twinned regions corresponding to the twin reflections are shown in Figs 9a and 9b, respectively.

Based upon the previous analysis of the deformation twins in ordered and deformed Ni_4Mo, and upon the fact that the stacking faults pass through both the matrix and the precipitates in the two-phase alloy, it is reasonable to conclude that the deformation twins in Figs 9a and 9b are composed of a series of stacking faults.

The deformation microstructure of an off-stoichiometric Ni–Ni_4Mo alloy therefore has the following characteristics as a function of aging time. At short aging times when only short-range order is present or when the ordered precipitates are sufficiently small, f.c.c. unit dislocations pass through the matrix phase, cutting the precipitates if the latter are present. When the precipitates are larger, f.c.c. partial dislocations and their attendant stacking faults pass through both the matrix and the precipitate phases. These stacking faults may in turn constitute deformation twins.

The Ni_4Mo superdislocation

In general the superdislocation of the ordered phase does not form in either the fully ordered stoichiometric alloy or in the off-stoichiometric alloy. However, occasionally groups of five dislocations per group were observed in the off-stoichiometric alloy, as shown in Fig. 10. These three groups of dislocations are followed by individual unit dislocations. All of the dislocations have identical Burgers vectors in the $[101]_\alpha$ direction as observed along the $[001]_\alpha$ zone

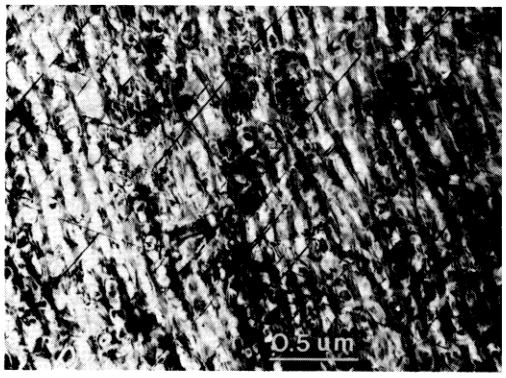

(a)

(b)

Fig. 9. (a) Bright-field micrograph of the deformation microstructure as observed along the $[001]_\alpha$ zone axis under multiple-beam diffracting conditions. (b) Dark-field micrograph of deformation twins produced by imaging a twin reflection.

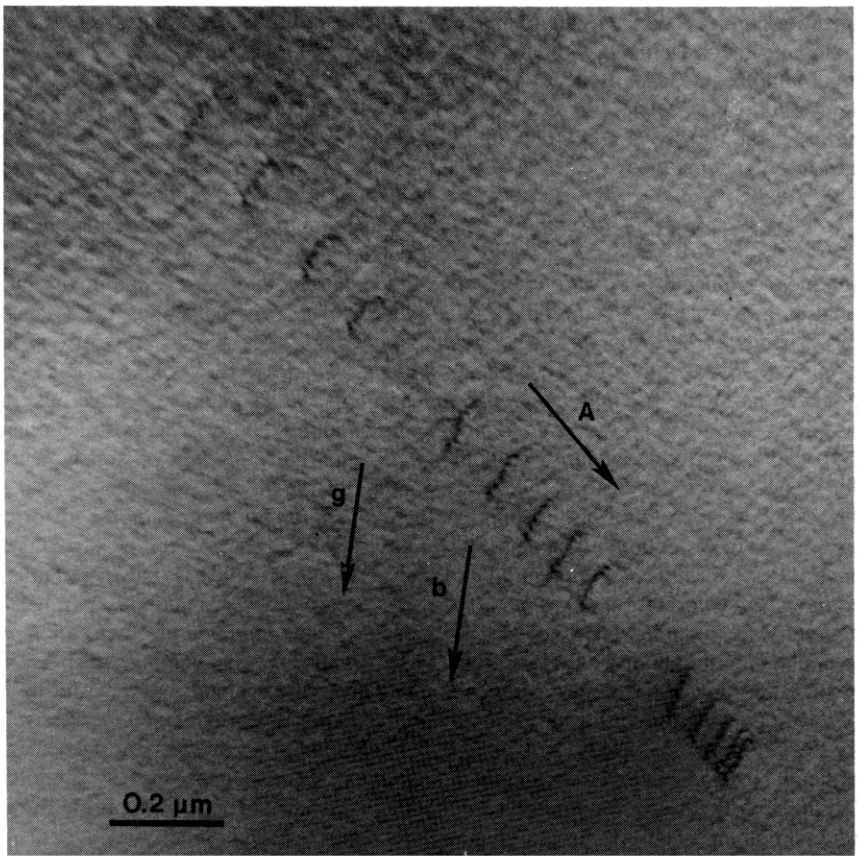

Fig. 10. Three superdislocations, each composed of 5 f.c.c. unit dislocations as observed in the off-stoichiometric alloy aged at 675°C (948 K) for 30 min. The operating diffraction conditions are $\mathbf{g} = [200]_\alpha$ along the $[001]_\alpha$ zone axis. The unit dislocations have Burgers vectors proportional to $[101]_\alpha$ and the projected direction of dislocation motions is parallel to the arrow marked 'A'. The projection of the $[101]_\alpha$ direction is indicated with the arrow marked 'b', and the direction of the g-vector is designated with an arrow marked 'g'.

axis. It was not possible to image the APB between the dislocations as the superlattice reflections were too weak and diffuse to permit the operation of a strong $\vec{\mathbf{g}} = 1/5\langle 420\rangle_\alpha$. The distribution of the unit dislocations indicates that three superdislocations are required to completely sever the Ni_4Mo precipitates so that the slip plane no longer lies within the precipitates, but only along the precipitate-matrix boundary. For a Burgers vector of $\vec{\mathbf{b}} = 1/2[101]_\alpha$, and using the lattice parameter values of Guthrie and Stansbury [19], the length of the Burgers vector for a unit dislocation is 0.254 nm. Thus the average precipitate diameter, d, can be approximated as

$$d = n|b| = 15(0.254) \approx 3.8 \text{ nm}$$

where n is the total number of unit dislocations in the identifiable superdislocations. Dark-field electron microscopy of the superlattice reflections reveals that the precipitates are 3–5 nm in size. This latter result is in good agreement with the precipitate size calculated from the above equation, and is consistent with the suggestion that the dislocations in Fig. 10 are f.c.c. unit dislocations, and that each group of five dislocations constitutes a superdislocation of the Ni_4Mo structure.

The separation between the unit dislocations within a superdislocation is the result of an energy balance among the self-energies of the dislocations, the interaction energy between the dislocations, and the antiphase boundary energy. For two identical, parallel unit dislocations, the first two energy contributions cause the unit dislocations to repel each other, while the third term (the APB energy) tends to hold the unit dislocations together at a fixed separation.

The change in the spacing between the unit dislocations within a superdislocation in Fig. 10 results from the dislocations shearing the ordered precipitates which traverse the slip plane. Each unit dislocation as it passes along the slip plane, not only cuts these precipitates, but also displaces the cut portions with respect to each other by one Burgers vector. This process reduces the total antiphase boundary area along the slip plane, while creating additional precipitate-matrix interfacial area. As a result the total antiphase boundary energy between unit dislocations is reduced. Thus as a superdislocation composed of more than

two unit dislocations moves along a slip plane the separation should be the least between the leading two dislocations and the greatest between the final two dislocations. From this analysis, the direction of motion of the dislocation array in Fig. 10 is in the direction of the accompanying arrow.

DISCUSSION

Probably the most significant observation concerning the deformation microstructure of the Ni–Ni_4Mo system is the general absence of an identifiable superdislocation both in the fully ordered stoichiometric alloy, as well as in the partially ordered off-stoichiometric alloy. (The three groups of 5 dislocations in Fig. 10 were a rarity.) The most probable explanation for this absence is the relative complexity of the superdislocation, since five unit dislocations are necessarily required for its formation. This complexity inhibits the nucleation of the full superdislocation as a discernible entity when deformation takes place at room temperature. Lakso and Marcinkowski [20] investigated a similar situation in ordered Fe_3Si (DO_3 structure) in which the superdislocation is composed of four unit dislocations. The superdislocations do not form at 243 K, but are present at 298 K. In the present case of ordered Ni_4Mo, a deformation temperature of 298 K is apparently too low for the nucleation of the superdislocation, which may form at higher deformation temperatures.

Recent work by Greggi and Soffa [21] on a Cu–Ti alloy, in which the Dla structure (Cu_4Ti) [22] also forms; indicates that deformation of that alloy at room temperature results in numerous superdislocations. These results and the general absence of superdislocations in our Ni–Mo alloy are consistent with the hypothesis proposed by Lakso and Marcinkowski [20], since the Cu–Ti alloy at room temperature is at a higher deformation temperature relative to its absolute melting point than is the Ni–Mo alloy.

Another significant observation concerning the deformation microstructure is the presence of large (wide) stacking faults in the ordered stoichiometric alloy (see Fig. 2) and also in the partially ordered off-stoichiometric alloy containing precipitates 80–100 nm in size (see Fig. 8). These stacking faults are not observed in the supersaturated or terminal solid solution and therefore the stacking fault energy of the ordered phase must be lower than that of the disordered solid solution.

In order to ascertain the reason for the prevalence of such stacking faults in the ordered or partially ordered structure, it is necessary to analyze the crystallographic effect of the passage of a partial dislocation on a slip plane compared to the movement of a unit dislocation. The movement of a unit dislocation with a Burgers vector of $\vec{b} = 1/2[110]_\alpha$ on the $(111)_\alpha$ plane through the ordered structure (Dla c-axis parallel to the $[001]_\alpha$ direction) results in a net change of four nearest neighbor Ni–Mo bonds to 2 Ni–Ni bonds and 2 Mo–Mo bonds over an area of approximately 0.56 nm^2. On the other hand, the passage of a partial dislocation with a Burgers vector of either $\vec{b} = 1/6[12\bar{1}]_\alpha$ on the same $(111)_\alpha$ plane does not result in any net change in the number of Ni–Mo bonds. However, a partial dislocation with $\vec{b} = 1/6[\bar{1}\bar{1}2]_\alpha$ would result in a net change in the number of such bonds. Since the movement of two of the three partial dislocations on a given close-packed plane does not create a net change in the number of each kind of near-neighbor bonds, the associated antiphase boundary energy should be relatively low. This particular characteristic of the Dla crystallography accounts, in part, for the numerous stacking faults observed in the fully ordered stoichiometric alloy and in the partially ordered off-stoichiometric alloy containing large Ni_4Mo precipitates.

An additional feature of the deformation microstructure with regard to the stacking faults in the ordered Ni_4Mo alloy is that these faults tend to form in overlapping groups on parallel close-packed planes, so as to constitute twins, or more specifically deformation twins. Venables [23] has demonstrated that a twinned crystal may be built up by a series of intrinsic stacking faults on successive close-packed planes in the f.c.c. lattice. This particular model inherently requires that these stacking faults be produced by partial dislocations of the same Burgers vector on each close-packed plane.

An unusual characteristic of such deformation twins in ordered Ni_4Mo is that if they are composed of the same partial dislocations which yield low energy stacking faults, then not only will these regions be twins of the f.c.c. lattice, but they will also be true crystallographic twins of the ordered Dla structure. That is, the twinned regions will retain the Dla structure although it will be of a different orientation variant than that of the untwinned region. In order to understand how such a twin might form, compare Fig. 11a with Fig. 1. Figure 11a shows the positions of the Mo atoms on three successive $(111)_\alpha$ planes. The triangles represent the Mo atoms in the lowest (bottom) plane, the circles indicate the positions of the Mo atoms in the middle plane, and the stars mark the Mo atom positions in the third or top plane. The projection of the Dla c-axis lies in the direction delineated by a triangle, a circle, and a star in succession. In Fig. 11a, the Dla c-axis is in the $[001]_\alpha$ direction and its projection is along the $[\bar{1}\bar{1}2]_\alpha$ direction.

Using the bottom $(111)_\alpha$ plane (the triangles) as a reference plane, let a partial dislocation of $\vec{b} = 1/6[\bar{1}2\bar{1}]_\alpha$ pass between the bottom and middle planes, thus shifting the Mo atoms on the middle and top planes (the circles and stars, respectively) in the $[\bar{1}2\bar{1}]_\alpha$ direction by $(a/\sqrt{6})_\alpha$. Now if an identical partial dislocation passes between the middle and the top planes, the Mo atoms on the top plane (the stars) will slip in the $[\bar{1}2\bar{1}]_\alpha$ direction again by $(a/\sqrt{6})$. The net result of these slips on successive $(111)_\alpha$ planes is shown in Fig. 11b. Again the Dla c-axis projects along

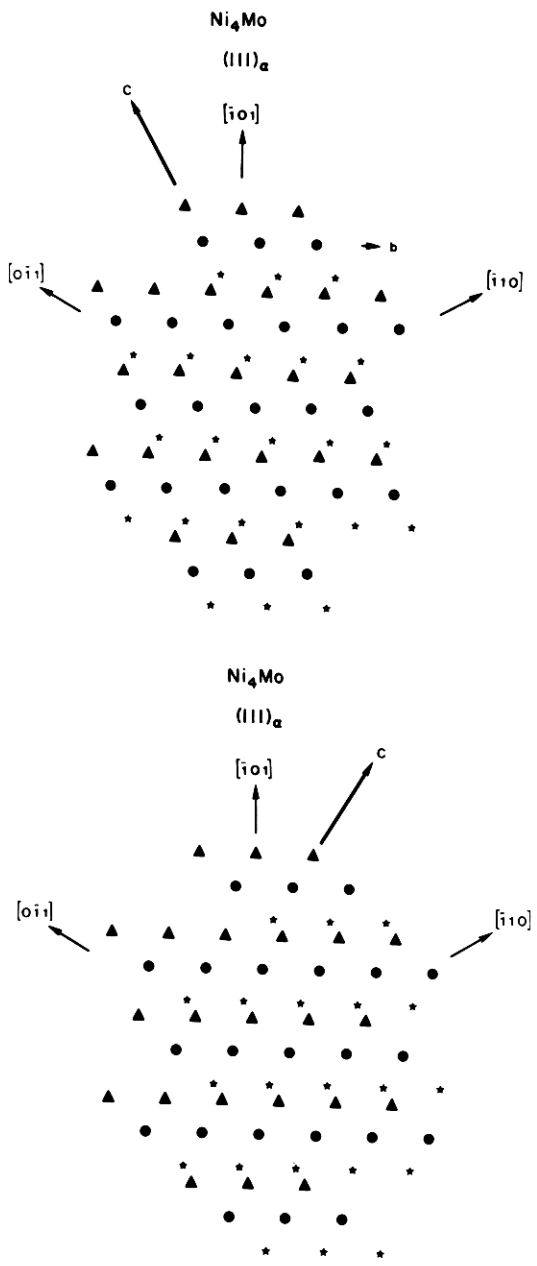

Fig. 11. The positions of the Mo atoms on three successive $(111)_\alpha$ planes is fully ordered Ni_4Mo, as designated by the triangles, circles, and the stars on the bottom, middle and top planes, respectively. (a) The positions of the Mo atoms prior to twinning. The arrow by the letter 'b' indicates the magnitude and direction of the $1/6[\bar{1}2\bar{1}]_\alpha$ partial dislocation which moves on successive $(111)_\alpha$ planes to form the twinned structure in (b).

the direction formed by a triangle, a circle and a star in succession, which in Fig. 12b is the $[\bar{2}11]_\alpha$ direction. However, this time its sense is changed, using the definition of Ruedl *et al.* [10] for the direction of the *c*-axis. Nevertheless, the region formed by the middle and top planes retains the Dla structure. It should be noted that the {111} twinning plane is not a mirror plane in this case. The atoms are reflected across the twinning plane *and* the $(\bar{1}2\bar{1})$ plane.

The fact that it is possible for the twinned region to retain the Dla structure and for the habit plane of the twin to be a low energy combination of stacking fault and perpendicular twin boundary, is consistent with the prevalence of deformation twins in the deformed microstructure of Ni_4Mo and of the off-stoichiometric alloy containing large precipitates.

Various models of dislocation mechanisms have been proposed which attempt to explain how deformation twins in general nucleate and grow within an alloy. Two basic approaches have been pursued in attempting to explain their formation. The first approach, as proposed by Orowan [24] envisages a twin embryo nucleating homogeneously in a region of high stress concentration. The second approach as developed by Venables [25], Cohen and Weertman [26], Hirth [27], and Mahajan and Chin [28] hypothesizes that the twin nucleates from a structural heterogeneity, such as a particular dislocation arrangement within the crystal.

The existing evidence from the deformation of both the stoichiometric and off-stoichiometric Ni–Mo alloys is that the stacking faults, which constitute the deformation twins, nucleate at grain boundaries and then move into the grains. Thus the deformation twins in the Ni–Ni_4Mo system nucleate at a structural heterogeneity.

CONCLUSION

The deformation microstructures of the stoichiometric Ni_4Mo alloy and of an off-stoichiometric Ni–Ni_4Mo alloy have several unique features which are due in part to the crystallography of the Dla (ordered Ni_4Mo) structure. In general the superdislocation does not form as an identifiable entity, even in the fully ordered stoichiometric alloy, when deformation takes place at room temperature. In these instances in which the superdislocation was observed, it consisted of five identical f.c.c. unit dislocations ($\vec{b}$ $1/2\langle 110\rangle_\alpha$). Wide, intrinsic stacking faults are also observed in the deformed microstructures of both the fully ordered Ni_4Mo alloy and of the off-stoichiometric alloy containing large precipitates, indicating that the stacking fault energy is considerably lower in the Ni_4Mo structure than in the disordered solid solution. This low stacking fault energy in the ordered phase is due to the fact that the passage of two of the possible three partial dislocations on a $\{111\}_\alpha$ close-packed plane does not change the number of each kind of first nearest-neighbor atom pairs across the slip plane. A third feature of the deformation microstructure is the formation of deformation twins composed of and formed by the aforementioned low energy stacking faults. Consequently the twinned regions retain the Dla structure of the untwinned region, albeit the twinned region is of a different orientation variant.

Acknowledgements—We would like to express our thanks and appreciation to Professor A. W. Thompson for reading an early draft of the paper and for making some helpful comments.

This research was sponsored by the National Science Foundation, Division of Materials Research, Grants 76-22353 and 78-05723.

REFERENCES

1. B. Chakravarti, E. A. Starke, C. J. Sparks, and R. O. Williams, *J. phys. Chem. Solids* **35,** 1317 (1974).
2. P. R. Okamoto and G. Thomas, *Acta Metall.* **19,** 825 (1971).
3. G. Van Tendeloo, *Mater. Sci. Engng.* **2a,** 209 (1976).
4. R. DeRidder, G. Van Tendeloo and S. Amelinckx, *Acta Crystallogr.* **A32,** 216 (1976).
5. S. K. Das, P. R. Okamoto, P. M. J. Fisher, and G. Thomas, *Acta Metall.* **21,** 913 (1973).
6. J.-P. Chevalies and W. M. Stobbs, *Acta Metall.* **27,** 1197 (1979).
7. L. E. Tanner and D. E. Laughlin, *Scripta Met.* **9,** 373 (1975).
8. L. A. Nesbit and D. E. Laughlin, *Acta Metall.* **26,** 815 (1978).
9. E. Ruedl, P. Delavignette and S. Amelinckx, *Phys. Stat. Sol.* **28,** 305 (1968).
10. E. Ruedl, P. Delavignette and S. Amelinckx, *Mater. Res. Bull.* **2,** 1045 (1967).
11. C. R. Brooks and F. E. Spruell, *Mater. Res. Bull.* **3,** 381 (1968).
12. B. Chakravarti, E. A. Starke, and B. G. LeFevre, *J. Mater. Sci.* **5,** 394 (1970).
13. J. W. Goodrum and B. G. LeFevre, *Metall. Trans.* **8A,** 939 (1977).
14. F. Laves, *Naturwissenschaften* **39,** 546 (1952); *Acta Metall.* **14,** 58 (1966).
15. ASTM Standard E8-69, *1976 Annual Book of ASTM Standards*, Part 10, ASTM, Philadelphia, PA. (1976).
16. R. Gevers, A. Art, and S. Amelinckx, *Phys. Stat. Sol.* **3,** 1563 (1963).
17. A. Art, R. Gevers, and S. Amelinckx, *Phys. Stat. Sol.* **3,** 697 (1963).
18. J. W. Edington, *Practical Electron Microscopy in Materials Science.* Van Nostrand Reinhold Company, New York (1976).
19. P. V. Guthrie and E. E. Stansbury, *ORNL 3078,* USAEC (1961).
20. G. E. Lakso and M. J. Marcinkowski, *Trans. AIME* **245,** 111 (1969).
21. J. Greggi, "*The Strength and Plastic Properties of Dilute Copper–Titanium Alloy Single Crystals,*" Ph.D. Thesis, University of Pittsburgh, Pittsburgh, Pennsylvania (1979).
22. D. E. Laughlin and J. W. Cahn, *Scripta Metall.* **8,** 75 (1974).
23. J. A. Venables, In *Deformation Twinning,* (Edited by R. E. Reed-Hill, J. P. Hirth, and H. C. Rogers), Gordon & Breach, New York (1964).
24. E. Orowan, in *Dislocations in Metals,* (Edited by M. Cohen) AIME, New York (1954).
25. J. A. Venables, *Phil. Mag.* **6,** 379 (1961).
26. J. B. Cohen and J. Weertman, *Acta Metall.* **11,** 997 (1963).
27. J. P. Hirth, In *Deformation Twinning,* (Edited by R. E. Reed-Hill, J. P. Hirth, and H. C. Rogers), Gordon & Breach, New York (1964).
28. S. Mahajan and G. Y. Chin, *Acta Metall.* **21,** 1353 (1973).